IEICE TRANS. COMMUN., VOL.E84–B, NO.11 NOVEMBER 2001

PAPER

A Novel Setup for Small Animal Exposure to Near Fields to Test Biological Effects of Cellular Telephones

Jianqing WANG† ***and*** **Osamu FUJIWARA**†**,** ***Regular Members***

SUMMARY A novel *in vivo* exposure setup has been developed for testing the possible promoting effects of 1.5 GHz digital cellular phones on mouse skin carcinogenesis. The exposure setup has two main features: one is the employment of an electrically short monopole antenna with capacitive-loading, which supplies the ability to realize a highly localized peak SAR above 2 W/kg without any thermal stress for a mouse; the other is the use of a transparent absorber to allow real-time observation of both the exposure process as well as mouse activities during the exposure. Dosimetric analyses for the exposure setup have been carried out both numerically and experimentally. Good agreement was confirmed between the numerical and experimental results, thereby demonstrating the validity of the novel exposure setup.

key words: *biological effect, cellular telephone, in vivo exposure setup, transparent absorber*

1. Introduction

With the recent rapid and ever more widespread use of cellular telephones, public concern regarding the possible health hazards has been growing. Although an extensive database exists for biological effects of electromagnetic waves, few are related to near-field exposure from cellular telephones. Definitive answers about the health hazards require further scientific studies, including *in vivo* animal experiments [1].

Since most experiments are done with rats and mice, various exposure systems have been or are being designed for the use of these species. The key point is to realize a specific absorption rate (SAR, expressed in watts per kilogram) in the tissue in relation to actual human exposure to cellular telephones. Four main types of exposure systems are available at the present time [2]–[8]. The first type is the use of an actual functioning cellular telephone. One problem with rats or mice, however, is their small size relative to the wavelength, which results in difficulties in realizing a localized exposure for these small animals. The second type involves making the SAR distribution pattern inside the small animals similar to that in the human head. The exposure frequency has to be scaled up by a factor equal to the ratio of human to animal size, which results in a much higher frequency than the actual frequencies of cellular telephones. The third type is the use of a loop antenna to irradiate the animal, which seems to be the most efficient for simulating a human exposure to cellular telephones because it gives a SAR distribution with a ratio of the peak to average SARs closest to the case occurring in a cellular telephone user. The fourth type is the use of a half-wavelength dipole or a quarter-wavelength monopole antenna radiating electromagnetic waves with the same frequencies and modulation waveforms as cellular telephones. The latter type of exposure system is the most popular at the present time, but the localized SAR can not be high enough relative to the whole-body-averaged SAR.

In Japan, the Association of Radio Industries and Businesses (ARIB) undertook an *in vivo* experimental project to investigate the effect of 1.5 GHz digital cellular telephones on carcinogenesis. Since the energy deposition from cellular telephones occurs mainly in human superficial tissue, the emphasis of this investigation was placed on testing possible promoting effects of cellular telephones on mouse skin carcinogenesis. To this end, ninety-six CD-1 mice were painted in a carcinogenic substance over a 1–2 cm^2 area in their superficial skin tissues and then divided into two groups: the EM field exposure group and sham group. The mice in EM field exposure group were locally exposed over 20–32 weeks and then the promoting effects on skin carcinogenesis were investigated. This paper focuses on the development of an appropriate exposure system and its numerical and experimental dosimetry evaluation.

2. Requirements

The basic requirement for the exposure system was to make the SAR distribution in a mouse as close as possible to that of a cellular telephone exposure actually occurring in a human. In fact, for a 1.5 GHz cellular telephone, the ratio of the ten-gram-averaged spatial peak SAR to the whole-head-averaged SAR was reported to be approximately 30 [9]. Similar results can be found for 900 MHz cellular telephones [10]. That is to say, to simulate an exposure from cellular telephones, a high SAR should occur in the mouse superficial tissue, and the whole-body-averaged SAR should be as low as possible in order not to cause any thermal stress. Of cause to expose a mouse to RF energy with a SAR distribution as close as possible to that of a cellular telephone,

Manuscript received February 8, 2001.
Manuscript revised June 7, 2001.

†The authors are with the Department of Electrical and Computer Engineering, Nagoya Institute of Technology, Nagoya-shi, 466-8555 Japan.

the local exposure should be in the mouse head. But due to the emphasis in this research being to locally expose the skin tissue, the exposure area was decided to be in the dorsal region from the point of view of convince of operation. It is known that there is no difference in biology for the skin tissue in the dorsal region and in the head region [11]. Therefore, paying attention to the superficial skin tissue, a system to expose the dorsal region of mouse is acceptable as long as a high SAR is realized in the skin tissue and a whole-body-averaged SAR is designed not to cause any thermal stress.

The Japanese Telecommunications Technology Council for the Ministry of Posts and Telecommunications has recommended that a localized SAR in humans should not exceed 2 W/kg averaged over any ten grams of tissue, and the whole-body-averaged SAR should not exceed 0.08 W/kg for a specified uncontrolled environment [12]. However, it is not realistic to apply a ten-gram average to a mouse for obtaining a peak SAR. There are no definite answers for how the ten-gram averaged peak SAR should be scaled from a human to a mouse. A conceivable method is to scale down the ten-gram in a human to a mouse according to the ratio of the human mass to the mouse mass, which yields a localized peak SAR of 2 W/kg averaged over 3–6 mg in a mouse. On the other hand, since the thermal threshold for mice is known to be 4–8 W/kg, a whole-body-averaged SAR of 0.08 W/kg for mice is unlikely to cause any thermal stress. Based on these considerations, the targets for the design of the exposure system were:

· a localized peak SAR above 2 W/kg in the skin

· a whole-body-averaged SAR below 0.08 W/kg as far as possible.

Figure 1 reviews the relationships between the localized peak SAR in the target tissue and the whole-body-averaged SAR for some *in vivo* exposure systems for small animals as reported recently. Chou et al. used a loop antenna, while the other investigators used a half-wavelength dipole or a quarter-wavelength monopole in their exposure systems, and the exposure target was the brain of rat or mouse. Except for Chou's result, the ratios of the peak SAR in the brain to whole-body-averaged SAR were found to be smaller than 9† even when a huge rat (Sprague-Dawley rat) was used [4]. These results imply the difficulty of a half-wavelength dipole or a quarter-wavelength monopole antenna in realizing our target of design for a mouse, whose size is much smaller than a rat, as shown in the dark area in Fig. 1.

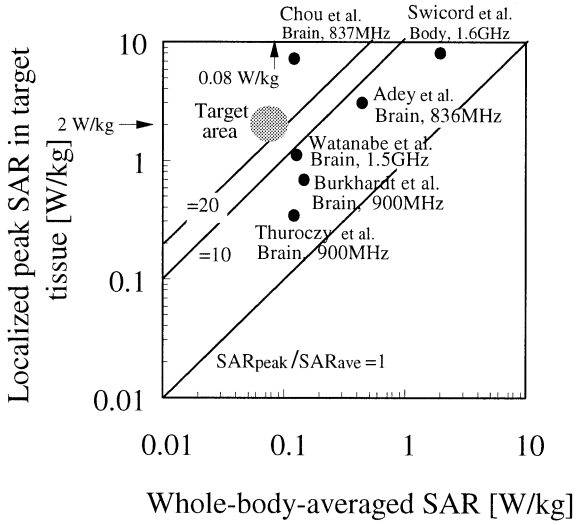

Fig. 1 Review of peak SAR and average SAR for the present exposure systems.

3. Exposure Antenna Design

3.1 Antenna Types

An electrically short antenna may be a means to realize the required exposure system. Figure 2 shows three possible types of exposure of a small animal: (a) monopole exposure, (b) dipole exposure with its element parallel to the longest axis of mouse, and (c) dipole exposure with its element perpendicular to the longest axis of mouse. The localized exposure area is the mouse dorsum. To obtain a preliminary evaluation for the three types of exposure, the dosimetry was first analyzed by the finite-difference time-domain (FDTD) method in conjunction with an approximate mouse model. The model was obtained by reducing the voxel size of a rat model, developed on the basis of an anatomical chart with a voxel size of 3 × 3 × 3 mm [3], to a new voxel size of 1.5 × 1.5 × 1.5 mm in order to obtain the size of mouse. The resultant model contains about 9,000 voxels and four types of tissue (skin, bone, muscle and liver) and is shown in the top of Fig. 2. The dielectric properties of each tissue, as described in [13], were accessed from a world wide web site at http://www.fcc.gov/fcc-bin/dielec.sh.

The whole computation domain enclosing the mouse model and the antenna consisted of about 3.6 million voxels. The use of such a large computation space may be inefficient from the point of view of computer memory but is useful to reduce the unwanted reflections in employing the second-order Mur absorbing boundaries to absorb the outgoing scattered waves. The antenna element with a radius of 0.4 mm was modeled by using the thin-wire approximation. An antenna excitation was introduced by specifying a sinusoidal voltage with an amplitude V across the one-cell gap, and the current flowing through the voltage source gap was then obtained from Ampere's law on a small curve

†Although the ratio of the peak SAR in the skin to the whole-body-averaged SAR would be larger, it decreases obviously when the animal is mouse whose size is much smaller than a rat.

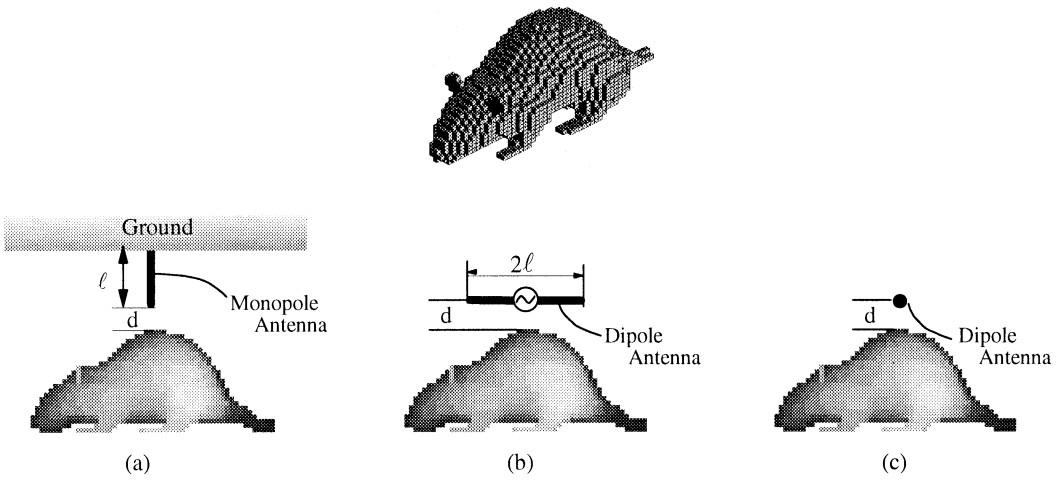

Fig. 2 Exposure types. (a) monopole exposure, (b) dipole exposure (parallel to the longest axis of mouse), (c) dipole exposure (perpendicular to the longest axis of mouse).

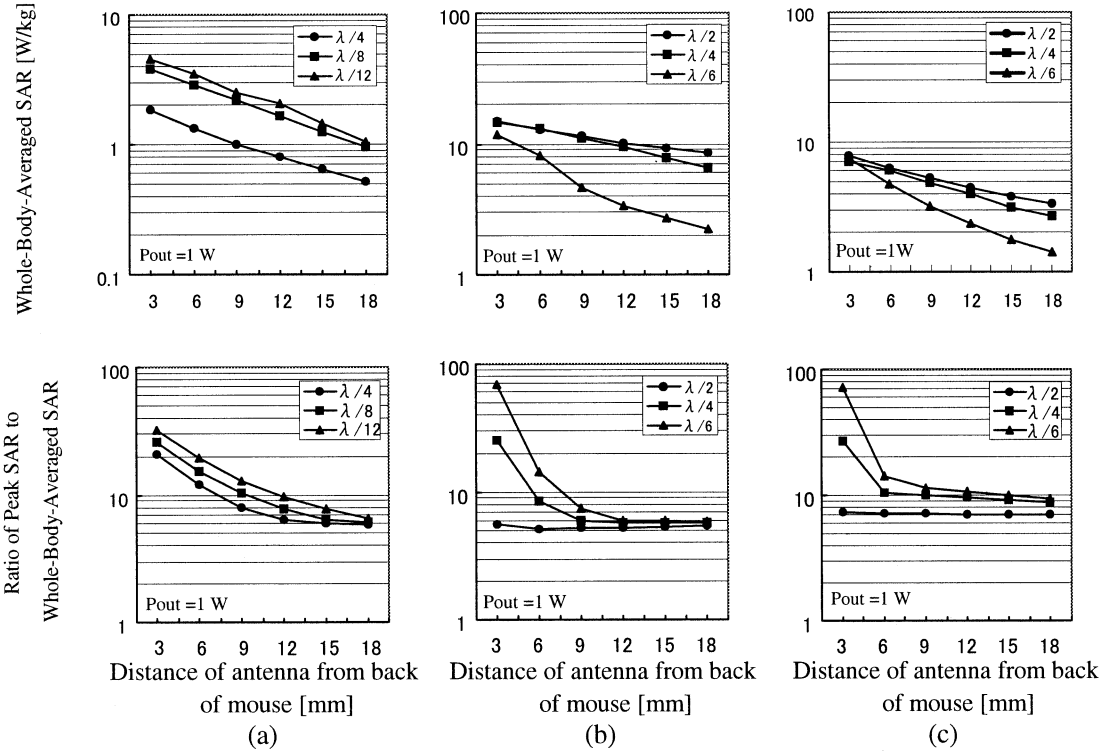

Fig. 3 Whole-body-averaged SAR (above) and ratio of the peak to whole-body-averaged SARs (below) for the mouse model. (a) monopole exposure, (b) dipole exposure (parallel), (c) dipole exposure (perpendicular).

around the gap. The output power of the antenna was calculated from

$$P_{out} = \frac{1}{2} Re\,(VI^*) \tag{1}$$

where I is the complex amplitude of the current, and $*$ denotes the complex conjugate. The SAR in each tissue voxel was computed by taking

$$SAR = \frac{\sigma}{2\rho}|E|^2 \tag{2}$$

where σ is the conductivity of tissue, ρ is the mass density assumed to be $1\,\mathrm{g/cm^3}$ for all types of tissue, and E is the electric field calculated from the 12 electric field components in the voxel.

Based on the consideration of mass scaling from human to mouse, as discussed in the previous section, the maximum SAR value in one voxel was used as the localized peak SAR because one voxel had a mass of about 3.4 mg. Figure 3 (above) shows the whole-body-

averaged SAR as functions of the distance between the antenna and the mouse as well as the length of the antenna element. For the monopole exposure, with shortening the length of antenna element, the feed-point of the monopole approached the animal and, as a result, the whole-body-averaged SAR increased, whereas, for the dipole exposure, shorting the length of antenna element yielded a smaller exposure area and then a decreased whole-body-averaged SAR. Figure 3 (below) shows the ratio of the localized peak SAR to the whole-body-averaged SAR as functions of the distance between the antenna and the mouse as well as the length of the antenna element. It was found that a ratio of 10–30 for the monopole exposure and a ratio of 5–70 for the dipole exposure were achieved at a distance smaller than 6 mm from the mouse. It is clear that the ratio of peak to average SARs are more distance-dependent for the dipole exposure. Table 1 gives the localized peak SAR when the whole-body-averaged SAR is 0.08 W/kg. A $\lambda/8$ monopole antenna or a $\lambda/4$ dipole antenna is available to realize a localized peak SAR of 2 W/kg at 3 mm from the mouse. Given the lower distance-dependence of the ratio of localized peak SAR to the whole-body-averaged SAR for the monopole exposure, the $\lambda/8$ monopole antenna seems to be more adequate. Figure 4 shows the SAR distribution on the surface of the mouse dorsum for the $\lambda/8$ monopole and $\lambda/4$ dipole exposure, which demonstrates that the $\lambda/8$ monopole gives a more localized exposure compared to the $\lambda/4$ dipole.

Table 1 Peak SAR relative to a whole-body-averaged SAR of 0.08 W/kg.

Exposure Type	Distance [mm]	Peak SAR [W/kg]
$\lambda/8$ monopole	3	2.06
	6	1.21
$\lambda/4$ dipole (parallel)	3	2.04
	6	0.68
$\lambda/4$ dipole (perpendicular)	3	2.13
	6	0.84

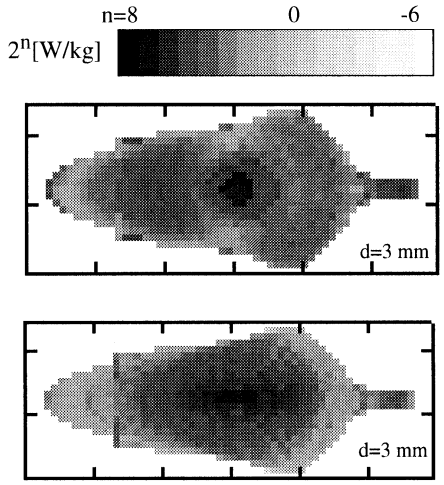

Fig. 4 SAR distribution on the surface of the mouse model. Above: $\lambda/8$ monopole exposure; below: $\lambda/4$ (parallel) dipole exposure. Antenna output was 1 W.

3.2 Exposure Power Efficiency

One problem using a short monopole antenna is the poor power delivered from the source to the antenna due to its small radiation resistance. In general, an animal experiment must be conducted on a large scale involving anywhere from 50 to 100 animals. This requires efficient delivery of power from the source to each antenna. To improve the exposure power efficiency of the antenna, a capacitive-loading (c-loading) $\lambda/8$ monopole antenna was designed with a metal circular plate having a diameter of 7 mm and a thickness of 1 mm attached to the top of the monopole element. Figure 5 shows the calculated power transmission coefficient (the reciprocal of mismatch loss) as a function of the distance from the mouse. The c-loading monopole antenna was found to significantly increase the antenna output. The radiation resistance increased from 15.8 Ω to 41.4 Ω at a distance of 3 mm from the mouse when the c-loading $\lambda/8$ monopole antenna was used. Moreover, the ratio of peak to average SARs as shown in Fig. 6 was not significantly changed, although the high SAR area was somewhat enlarged on the mouse dorsum for the c-loading short antenna. As a result, to realize a peak SAR of 2 W/kg at a distance of 3 mm from the mouse, the input power required for the antenna is below 30 mW. It should be noted that due to the capacitive loading the highest one-voxel SAR value was moved from the location just beneath the tip of the monopole to the location beneath the edge of the circular plate (referring to Fig. 4(a) and Fig. 12(b)).

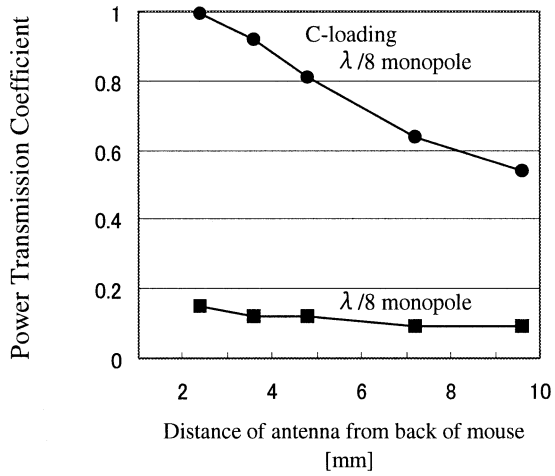

Fig. 5 Power transmission coefficient for short monopole antennas.

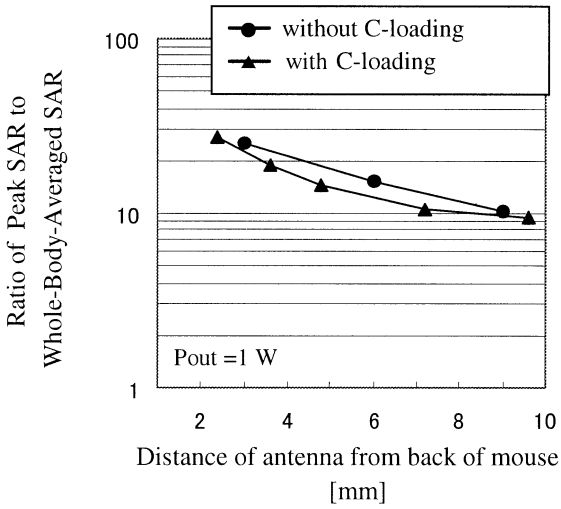

Fig. 6 Ratio of the peak to whole-body-averaged SARs.

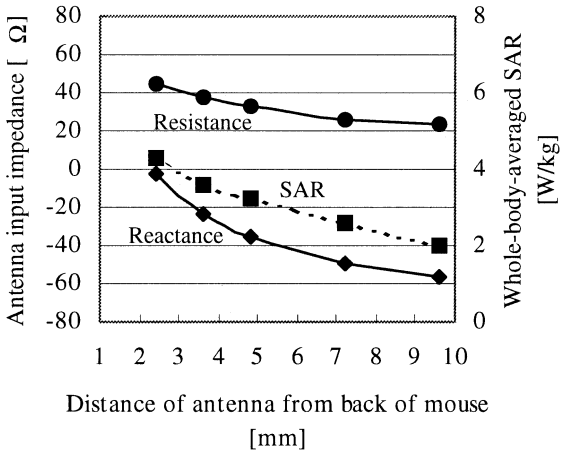

Fig. 7 Relationship between the whole-body-averaged SAR and antenna input impedance.

3.3 Dependence of SAR on Antenna Impedance

The dependence of the SAR on antenna impedance is helpful to understand the mechanism of interaction between the c-loading antenna and the mouse for the exposure setup. Figure 7 shows the FDTD-computed input impedance of the c-loading antenna as a function of the distance from the mouse. Also shown in Fig. 7 is the whole-body-averaged SAR in the mouse also as a function of the distance of antenna from the mouse. From this figure the dependence of the absorption on the input impedance of the antenna can be extracted, which suggests that keeping the antenna feeding current constant will result in a more rapidly decrease for the SAR with the distance from the mouse.

4. Exposure Box Design

A prototype of the exposure box is shown in Fig. 8.

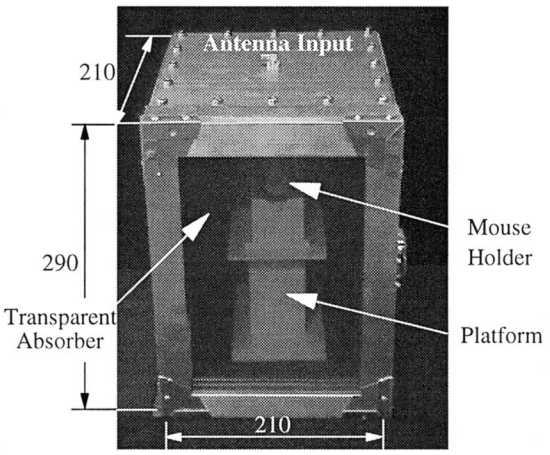

Fig. 8 View from front door with transparent absorber of exposure box.

The box is made of aluminum, and its insides, except for the roof and the front door, are inlaid with planar rubber ferrite absorber having a thickness of 7 mm and a reflection loss of at least 21.8 dB at 1.5 GHz. The roof of the box acts as the ground for the c-loading $\lambda/8$ monopole antenna which is fed at the center of the roof. The front door is a new type absorber—transparent absorber (developed by TDK Corporation) with a thickness of 22.5 mm and able to supply a reflection loss of about 20 dB. The transparent absorber allows real-time observation of the exposure process as well as mouse activities. As can be seen from Fig. 8, the degree of transparency of the transparent absorber was satisfactory. Inside the exposure box, an acrylic holder was set on a plastic platform to restrain the mouse so that its dorsum is positioned just beneath the exposure antenna. The distance between the mouse holder and the antenna is set by adjusting the height of the plastic platform. The mouse holder has more than 10 holes on its ends and sides to provide the mouse with ventilation. An air hose with a diameter of 3 mm is set in the vicinity of the nose of the mouse. The air hose delivers fresh air at 3 levels, and the maximum air flow is 6 l/min. Because a typical adult mouse requires minimal ventilation smaller than the order of 0.125 l/min, an air flow of 6 l/min at most is considered to be sufficient.

The size of the exposure box was determined by computing the SAR of the mouse model in various-sized boxes using the FDTD method. In the computation, both the rubber ferrite absorber and the transparent absorber were modeled with their complex permeability and complex permittivity. Computed results show that such a box with sides more than 15 cm wide and over 12 cm high can give almost the same peak and whole-body-averaged SAR values as that in a semi-infinite space. Based on the simulation result and for easy insertion/removal of the mouse, the prototype exposure box was designed to have internal dimensions of 21 ×

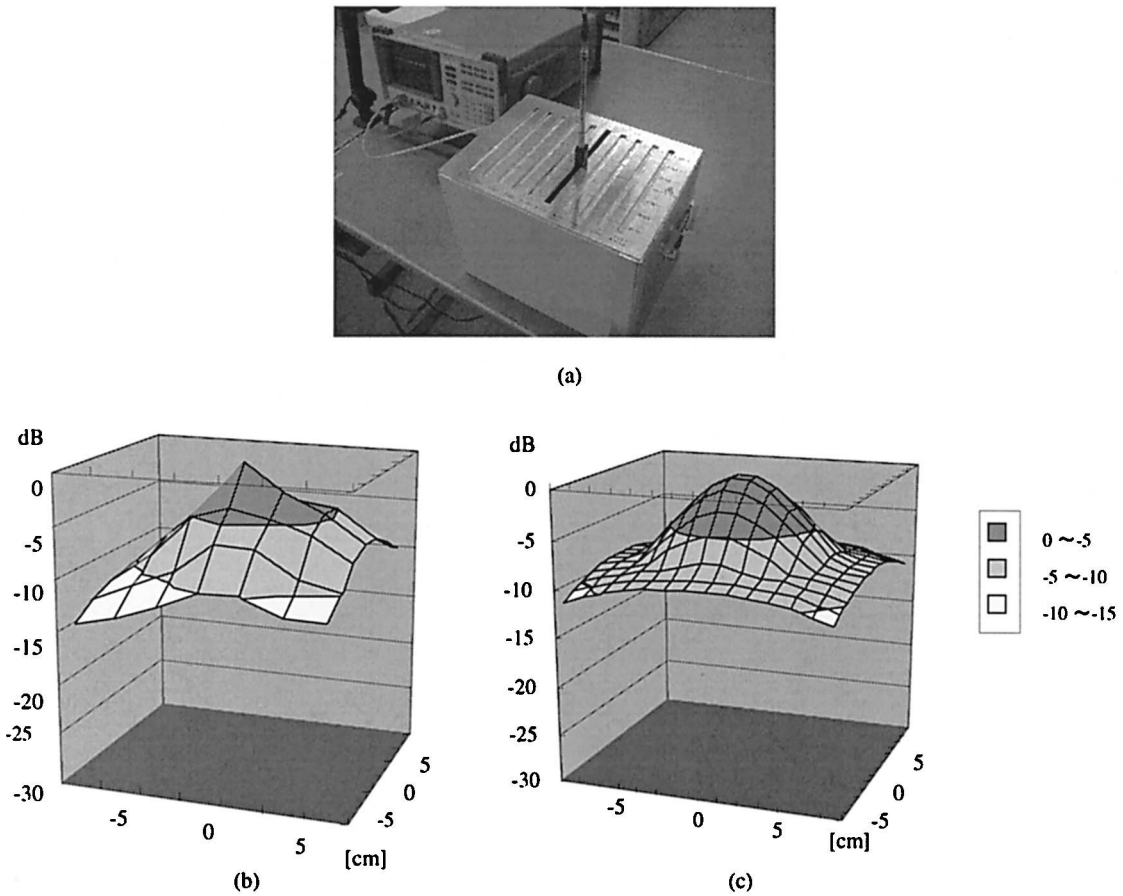

Fig. 9 (a) View of measurement, (b) measured electric field distribution and (c) computed electric field distribution at a horizontal plane in the exposure box with a distance of 3.7 cm from the antenna.

21 × 29 cm.

5. Dosimetry Evaluation

5.1 Field Distribution

It is meaning to first measure the actual EM field distribution in the box at the exposure volume without the mouse and platform and compare it with the computed values using the FDTD model. As shown in Fig. 9(a), the measurement was performed by replacing a side of the exposure box with a aluminum plate inlaid with a planar rubber ferrite absorber. The ferrite-absorber-inlaid aluminum plate was processed to have many slits. The electric field (vertical component) distribution was measured by inserting a standard dipole probe into the box from these slits. Figures 9(b) and (c) show the measured and FDTD-computed results in the horizontal plane at a distance of 3.7 cm from the antenna, which gives a fair agreement between the measurement and computation. The results also show that the absorber employed in the exposure box indeed possessed a considerably large reflection loss at 1.5 GHz so that the reflections from them were almost insignificant.

5.2 Dosimetry

The dosimetry evaluations for the prototype exposure setup were carried out both experimentally and numerically. A detailed numerical model, as shown in Fig. 10(a), was used in the numerical dosimetry evaluation. The original model was derived from 81 magnetic resonance images (MRI) taken from a Sprague-Dawley rat by Dr. Mason et al. and was accessed from http://www.brooks.af.mil. In the present study, it was rescaled to a voxel size of 1.2 × 1.2 × 1.2 mm (about 1.7 mg) in order to be mouse size, which resulted in about 14,700 voxels and 20 types of tissue. In such a way, the obtained mouse model had a thickness of 1.2 mm for the target tissue of interest, i.e., the skin. In fact, the skin is at least composed of three layers: the epidermis, dermis and subcutaneous tissue. Based on our anatomical result for the CD-1 mice used in the experiment, the thickness of skin for these species is on the order of 1 mm, which suggests that the mouse model is valid for the present purpose. The computed ratio of the peak to whole-body-averaged SARs for the detailed model was first compared with the previous ap-

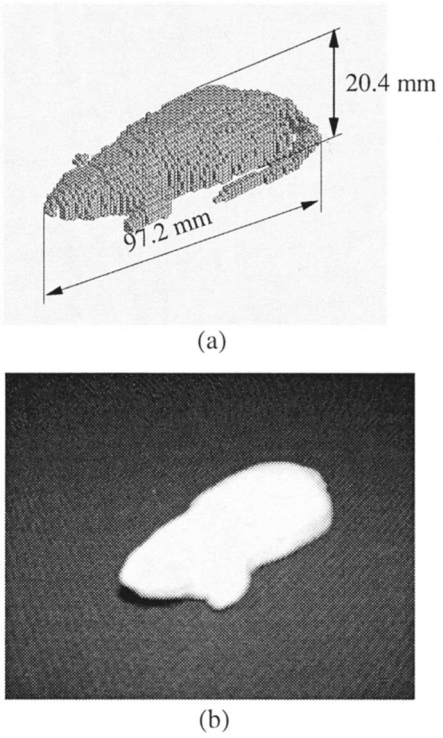

Fig. 10 (a) Detailed numerical mouse model, (b) solid mouse phantom.

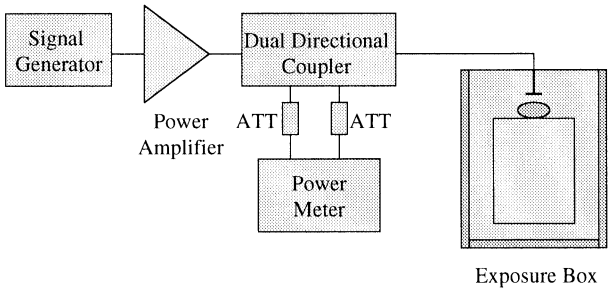

Signal Generator: HP ESG-D300A
Dual Directional Coupler: HP778D
Power Meter: HP EPM-442A + HP8482A
Power Amplifier: Max 50W
ATT: 30dB

Fig. 11 Experimental setup for dosimetry evaluation.

proximate model, and the difference between them was within 10%. This finding suggests that the dependence of the peak SAR on animal modeling is insignificant, which may be attributed to the fact that the exposure target is superficial skin tissue.

For the experimental dosimetry evaluation, homogeneous solid (gel with agar added) phantoms having the same shape as the above-detailed model were used (see Fig. 10(b)). Their conductivity and relative permittivity proved to be 2.1 S/m and 54.53, respectively, using a network analyzer and a dielectric probe kit (HP8753A + HP85046A). Figure 11 shows the experimental setup for dosimetry evaluation. The radiated antenna power was 40 W, and the mouse phantom was exposed for 30 seconds. The SAR in the mouse phantom was measured with two methods, both of which assumed linear energy deposition within the 30-second period. In the first method, flour-optic temperature probes (Luxtron, Model SMM) were inserted into the phantom and set at four locations along the vertical line under the exposure antenna at 5-mm intervals, or at three locations at 2-cm intervals along the horizontal center line at the surface of the phantom. The temperature reading at each location was recorded every second over the 30-second period. Then the SAR at each location was determined from

$$SAR = C_p \frac{dT}{dt} \simeq C_p \frac{\Delta T}{\Delta t} \tag{3}$$

where C_p is the specific heat [J/kg·℃], ΔT is the temperature-rise due to the exposure, and Δt is the exposure time. The value of C_p was taken to be 3725 J/kg·℃ [14] which was identical to the data measured by using a commercially available specific heat measuring apparatus. The exposure was repeated two to three times, and in each a new mouse phantom was used.

The second method was performed similar to the first, but an infrared image camera was used in lieu of the temperature probes. The mouse phantom before exposure was first set close to the ambient temperature, and the corresponding infrared image was recorded. After the 30-second exposure, the mouse phantom was immediately removed from the exposure box and the infrared image was obtained again. Then the temperature-rise at the phantom surface was obtained from their difference, and the SAR was determined in the same way as in the first.

Figure 12 shows the infrared image (temperature distribution) at the surface of mouse phantom along with the FDTD-computed SAR distribution. A very similar pattern can be observed between them. Figure 13 shows measured SAR along the vertical line under the exposure antenna, and Fig. 14 shows it along the horizontal center line at the surface of the phantom. Also shown in the figures with a solid line is the SAR computed by using the FDTD method in conjunction with the same homogeneous model. For the SAR inside the phantom, both the temperature probe method and the infrared image method gave very good agreement with the FDTD computation. For the SAR at the target area, i.e., the superficial tissue, a good agreement was observed between the average of measurements and computation, say just 5% lower for the temperature probe method and 10% lower for the infrared image method than the FDTD computation. The good agreement among the two measurements and FDTD computation assured the reliability of our dosimetric analysis. The reason why the measured surface SAR was slightly lower than computed ones may be due to the influence

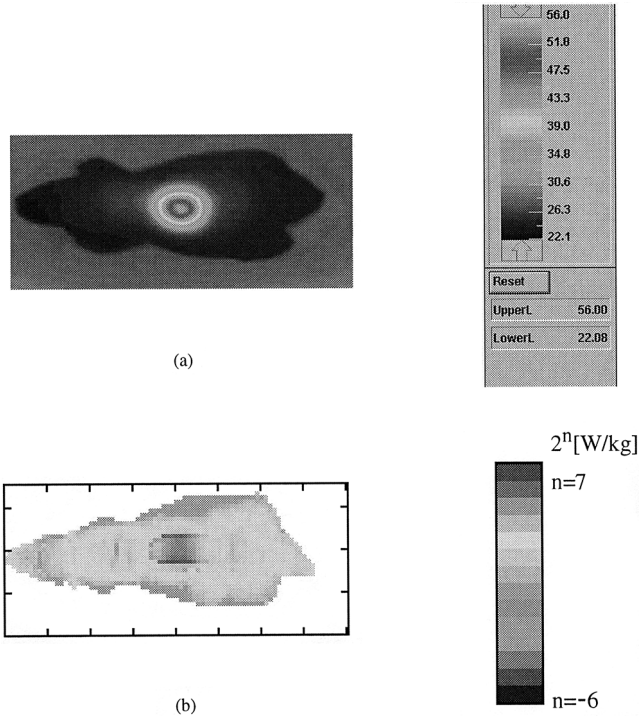

Fig. 12 (a) Measured infrared image with an antenna output of 40 W, and (b) computed SAR distribution for antenna output of 1 W at the surface of mouse phantom.

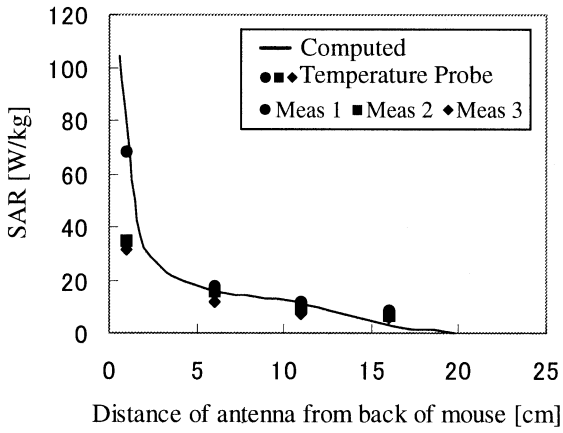

Fig. 13 SAR distribution along the vertical line under the exposure antenna. Antenna output was normalized to 1 W. The distance between the antenna and the phantom was 3 mm.

of the heat transfer to air. First, the 30-second exposure period was not short enough to prevent the heat transfer from the phantom surface to air. To shorten the exposure time and consequently reduce the influence of heat transfer to air, a higher output for the power amplifier is required. Second, in the infrared image method, the mouse phantom had to be removed from the exposure box for temperature measurement. This process required several seconds, and the heat transfer to air during this period resulted in a larger error in comparison with the temperature probe method. An-

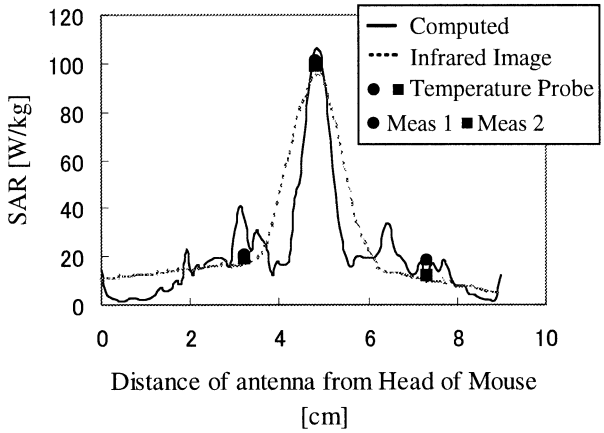

Fig. 14 SAR distribution along the horizontal center line at the superficial layer of phantom. Antenna output was normalized to 1 W. The distance between the antenna and the phantom was 3 mm.

Table 2 Peak and whole-body averaged SARs in exposure box.

Peak SAR	2.0 [W/kg]
Whole-body-averaged SAR	0.084 [W/kg]
Ratio of peak to average SARs	24

Antenna output : 23 mW

other possible reason is the inherent artifact in FDTD modeling for irregular surfaces with rectangular cells, which may yield an overestimate for the SAR values in that cells, as described in [7]. As for the large variation of the experiment data at 1 cm distance from the back of the mouse in Fig. 13, it is considered to be due to the location error in setting the temperature probe because it is not easy to fix the probe in the superficial layer of phantom.

Table 2 gives computed peak SAR and whole-body-averaged SAR for the detailed heterogeneous mouse model in the exposure box with a distance of 3 mm from the antenna. The peak SAR was calculated from the average of two voxels in the skin tissue for obtaining an localized SAR over 3.4 mg and normalized to be 2 W/kg. As can be seen from Table 2, our target of design as shown in Fig. 1 was realized by using the prototype exposure setup.

5.3 Effect of Mouse Movement

Since the peak SAR varies drastically with the distance between the mouse and the antenna in the vicinity of a 3 mm distance, it is necessary for this exposure setup to effectively constrain the mouse with a holder. Although so, a limited movement of the mouse inside the holder is still possible, which would influence the antenna input impedance and consequenctly result in an antenna power variation. For investigating the power variation due to the mouse movement, six CD-1 mice with weights ranged from 27 to 38 grams were used. Each of them was constrained in an acrylic holder as

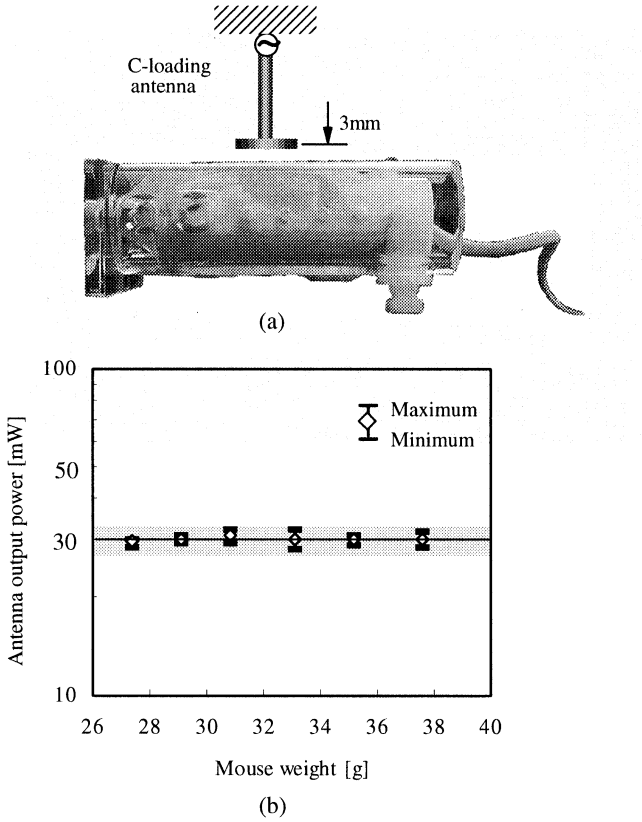

Fig. 15 Variations of antenna output power as a function of weight for mouse.

shown in Fig. 15(a) and placed in the exposure box respectively. The height of the platform was adjusted so that the distance between the back of the mouse and the antenna was 3 mm. The c-loading antenna was fed by a signal generator (Anritsu MG3670B), and the antenna output power was measured using two power meters (Anritsu ML4803A, MA4601A sensor) from the difference between the incident power to the antenna and the reflected power from the antenna. Each measurement was conducted for 80 minutes and the outputs from the power meters were recorded in a one-second interval. Figure 15(b) shows the measured variations of the antenna output power for the six mice. The variations of the antenna output power were found to be within $\pm 7\%$ due to the movement of mouse in the holder. It should be noted that the variation of the antenna output power is the sum of the variations of the powers absorbed in the mouse and the absorbing material of exposure box. Directly linking it to the SAR variation in the mouse is difficult in the present method, which requires further studies.

6. Conclusion

In this work, we developed a novel exposure setup to test for possible promoting effects of 1.5 GHz digital cellular phones on mouse skin carcinogenesis. The exposure setup has two main features, one of which is the employment of an electrically short monopole antenna with capacitive-loading. The antenna makes it possible to realize a localized peak SAR above 2 W/kg without any thermal stress for a mouse, enabling simulation of human exposure to RF fields from a cellular telephone. Another feature is the adoption of a transparent absorber for real-time observation of both the exposure process as well as mouse activities. Dosimetric analyses for the exposure setup were carried out both numerically and experimentally. Good agreement was found between the numerical and experimental results, demonstrating the validity of the novel exposure setup.

Further studies will attempt to evaluate the uncertainty in the SAR assessment, especially for the localized peak SAR in the exposure setup.

Acknowledgment

This study was performed with support from the Association of Radio Industries and Businesses (ARIB), Japan. The authors would like to thank Dr. Y. Hashimoto, TDK Corporation, for his contribution to the exposure box with transparent absorber, Dr. S. Watanabe, Communications Research Laboratory, Japan, for his help in the dosimetric experiment, and Prof. S. Tokumaru, Keio University, Japan, for his constructive discussions with us on the antenna designs. The authors would also like to thank Dr. P.A. Mason, Air Force Research Laboratory, Brooks AFB, Texas, USA, and Prof. M. Taki, Tokyo Metropolitan University, Japan, for providing the small animal models.

References

[1] The International EMF Project, "Electromagnetic fields and public health," WHO Fact Sheets 181, World Health Organization (WHO), Geneva, 1998.
[2] G. Thuroczy, J. Bakos, and L.D. Szabo, "Practical considerations in bioelectromagnetics dosimetry: SAR measurement of RF and microwave exposure in animal phantoms related to mobile phones," Proc. COST 244, pp.104–110, Athens, 1995.
[3] M. Burkhardt, Y. Spinelli, and N. Kuster, "Exposure setup to test effects of wireless communications systems on the CNS," Health Physics, vol.73, pp.770–778, 1997.
[4] S. Watanabe, Y. Yamanaka, and M. Taki, "An exposure setup for *in vivo* studies to test biological effects in a head locally exposed to MW from a cellular telephone," IEICE Technical Report, EMCJ98-42, 1998.
[5] E.G. Moros, W.L. Straube, and W.F. Plckard, "A compact shielded exposure system for the simultaneous long-term UHF irradiation of forty small mammals: I. Electromagnetic and environmental design," Bioelectromagnetics, vol.19, pp.459–468, 1998.
[6] M. Swicord, J. Morrissey, D. Zakharia, M. Ballen, and Q. Balzano, "Dosimetry in mice exposed to 1.6 GHz microwaves in a carrousel irradiator," Bioelectromagnetics, vol.20, pp.42–47, 1999.
[7] C.K. Chou, K.W. Chan, J.A. McDougall, and A.W. Guy,

"Development of a rat head exposure system for simulating human exposure to RF fields from handheld wireless telephones," Bioelectromagnetics, vol.20, pp.75–92, 1999.

[8] W.R. Adey, C.V. Byus, C.D. Cain, R.J. Higgins, R.A. Jones, C.J. Kean, N. Kuster, A. MacMurray, R.B. Stagg, G. Zimmerman, J.L. Phillips, and W. Haggren, "Spontaneous and nitrosurea-induced primary tumors of the central nervous system in Fischer 344 rats chronically exposed to 836 MHz modulated microwaves," Radiation Research, vol.152, pp.293–302, 1999.

[9] J. Wang and O. Fujiwara, "FDTD computation of temperature-rise in the human head for portable telephones," IEEE Trans. Microwave Theory & Tech., vol.47, no.8, pp.1528–1534, Aug. 1999.

[10] M. Okoniewski and M.A. Stuchly, "A study of the handset antenna and human body interaction," IEEE Trans. Microwave Theory & Tech., vol.44, no.10, pp.1855–1864, Oct. 1996.

[11] G.A. Boorman, S.L. Eustis, M.R. Elwell, C.A. Montgomery, Jr., and W.F. MacKenzie, eds., Pathology of the Fischer Rats, pp.261–278, Academic Press Inc., San Diego, 1990.

[12] Telecommunications Technology Council for the Ministry of Posts and Telecommunications, Deliberation no.89, "Radioradiation protection guidelines for human exposure to electromagnetic fields," Tokyo, 1997.

[13] C. Gabriel, "Compilation of the dielectric properties of body tissues at RF and microwave frequencies," Brooks Air Force Technical Report AL/OE-TR-1996-0037, 1996.

[14] J. Hardy, A. Gagge, and J. Stolwijh, eds., Physiological and Behavioral Temperature Regulation, pp.281–301 & pp.345–357, Thomas, Springfield, IL., 1970.

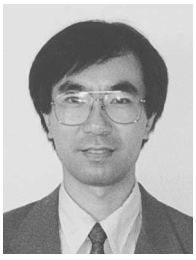

Jianqing Wang received the B.E. degree in electronic engineering from Beijing Institute of Technology, Beijing, China, in 1984, and the M.E. and D.E. degrees in electrical and communication engineering from Tohoku University, Sendai, Japan, in 1988 and 1991, respectively. He was a Research Associate at Tohoku University and a Research Engineer at Sophia Systems Co., Ltd., prior to joining the Department of Electrical and Computer Engineering, Nagoya Institute of Technology, Nagoya, Japan, in 1997, where he is currently an Assistant Professor. His research interests include electromagnetic compatibility, bioelectromagnetics and digital communications.

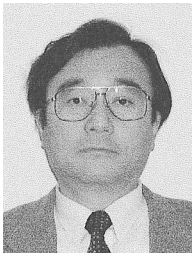

Osamu Fujiwara received the B.E. degree in electronic engineering from Nagoya Institute of Technology, Nagoya, Japan, in 1971, and the M.E. and the D.E. degrees in electrical engineering from Nagoya University, Nagoya, Japan, in 1973 and in 1980, respectively. From 1973 to 1976, he worked in the Central Research Laboratory, Hitachi, Ltd., Kokubunji, Japan, where he was engaged in research and development of system packaging designs for computers. From 1980 to 1984 he was with the Department of Electrical Engineering at Nagoya University. In 1984 he moved to the Department of Electrical and Computer Engineering at Nagoya Institute of Technology, where he is presently a professor. His research interests include measurement and control of electromagnetic interference due to discharge, bioelectromagnetics and other related areas of electromagnetic compatibility. Dr. Fujiwara is a member of the IEE of Japan and of the IEEE.